Trans Indian Inst Met
DOI 10.1007/s12666-015-0691-9

TECHNICAL PAPER

Microstructural, Magnetic and Electrical Properties of Ni_2FeGa Heusler Alloys

Hrusikesh Nath[1] · **G. Phanikumar**[1]

Received: 27 May 2015 / Accepted: 20 August 2015

Abstract Ni_2FeGa polycrystalline alloys are synthesized by arc melting into single phase β structure and two phase mixture of γ-phase (fcc) and austenite (L_{21}). Annealing improves atomic ordering and β transforms to L_{21} ordered structure. Effect of alloy composition and processing condition on different phase formation, microstructural, magnetic and electrical properties are discussed. The alloy undergoes first order austenite to martensitic phase transformation at 225 K with low hysteresis of 10 K. The resistivity exhibits a jump upon martensite transformation. This increase in resistivity is being attributed to the change in effective mass of electron upon martensite transformation. The temperature dependent resistivity curve for both austenite and martensite varies linearly with αT suggesting strong electron–phonon scattering. The slope of temperature dependent resistivity curve is higher in case of austenite than that of martensite and is attributed to the increasing role of electron–phonon scattering at high temperature.

Keywords Heat treatment · Magnetization · Martensite transformation · Resistivity

✉ Hrusikesh Nath
hrushikesh.nath@gmail.com

G. Phanikumar
gphani@iitm.ac.in

[1] Department of Metallurgical and Materials Engineering, Indian Institute of Technology Madras, Chennai 600036, India

1 Introduction

In recent decades, many literatures have been published on Ni–Fe–Ga Heusler alloy system for the investigation of magnetic shape memory effect. Huang et al. [1] have reported the shape memory properties of Ni_2FeGa Heusler alloys. They have shown complete pseudoelastic recovery of 5 % in highly oriented polycrystalline Ni–Fe–Ga alloys. Ductility and hot deformation behavior get improved with the presence of γ-phase in the microstructure [2]. The traces of γ-phase in the matrix of the microstructure of single crystal Ni_2FeGa generates residual stress which results in two way shape memory effect [3]. The functionality of shape memory alloys largely depend on various aspects of martensitic transformation such as transformation temperature (T_m), elastic energy stored due to transformation, structure of martensite, the type of variants formed and their morphology. The mentioned properties are closely related to the high temperature phase austenite, its structure, chemical composition, grain size, degree of atomic ordering and the magnetic properties [4–7]. In case of Heusler alloys, the magnetic state of martensite and the magnetic anisotropic properties also influence the functional properties. Hence in this article, we investigated the effect of alloy composition and processing conditions on different phase formation and martensite transformation in Ni_2FeGa Heusler alloy. It was possible to synthesize single austenite phase in bulk alloy sample near Heusler stoichiometry in Ni–Fe–Ga system unlike the formation of single austenite phase in previously reported melt spun ribbons of Ni_2FeGa samples. High cooling rate associated with chilled Cu-hearth in arc melting process and higher Ga content in alloy composition was able to suppress γ-phase formation and synthesize single austenite phase. The structural ordering upon annealing of alloy sample was also investigated.

Published online: 14 November 2015

Modulated martensite structures in Ni_2FeGa Heusler alloys have also been reported elsewhere. Microtwins within martensite lamellae were observed by Liu et al. [8], which were induced due to high internal stress in the vicinity of grain boundaries. Thus, high temperature phase formation and martensite transformation are crucial in Ni–Fe–Ga system for future shape memory application. Reversible martensite transformation with low hysteresis is an essential component required for shape memory effect. Low activation energy of martensite transformation coupled with high stacking fault energy led to the martensite transformation with little irreversibility [9]. Thus in this article, the reversibility of martensite transformation with low hysteresis was established by DSC and electrical resistivity measurement. The behavior of resistivity upon martensite transformation was compared with the existing literature data to understand the transformation in more detail.

2 Materials and Methods

Ni_2FeGa Heusler alloys were prepared by arc melting in argon atmosphere by choosing the nominal stoichiometry X_2YZ. The chamber was evacuated to 10^{-5} bar, backfilled with argon and the alloys were cast into button shape (approximately 4 g) using chilled Cu-hearth. The alloys were melted four times to promote compositional homogeneity. Three different Ni_2FeGa alloys were prepared and referred to as alloy-a, alloy-b and alloy-c (see Table 1). All the alloys were sealed inside an evacuated (10^{-5} bar) quartz tube separately, homogenized at 1273 K for 1 h and quenched in water. Alloy-a and alloy-b were annealed at 1073 K and alloy-c at 773 K for 1 h each and slowly cooled to room temperature to promote atomic ordering. The second stage annealing improved the chemical ordering which further increased the martensitic transformation temperature. The microstructural properties were studied using X-ray diffraction, electron microscopy. The phase transformation behavior was investigated by differential scanning calorimeter at heating/cooling rate of 10 K/min in the temperature range of 148–373 K (−125 to +100 °C) and the room temperature magnetic properties were studied using vibrating sample magnetometer. Temperature dependent electrical resistivity was measured by four probe technique using rectangular shaped sample with dimension 2 mm × 2 mm × 8 mm. Heating/cooling rate of 2 K/min in the temperature range of 20–300 K was adopted to investigate the martensite transformation and the electrical transport properties of Ni_2FeGa Heusler alloy-b.

3 Results

The two phases in alloy-a and alloy-b were identified to be γ-phase and austenite with fcc and L_{21} structures respectively (Fig. 1). The XRD patterns in Fig. 1a show the structures of alloy-a and alloy-b after second stage annealing process. The peaks corresponding to the L_{21} structure are clearly identified in both the patterns. In austenite phase, all the three elements (Ni, Fe and Ga) form L_{21} ordered structure by occupying their respective lattice positions. The amount of chemical ordering present in the high temperature phase affects martensitic transformation. Alloy-a maintains the stoichiometry close to X_2YZ Heusler composition. Alloy-b has higher Ni-content, deliberately added replacing Ga to see the changes in martensitic transformation temperature. There are many reports on off-stoichiometric composition to induce chemical disorder in the material [10, 11]. The composition of the alloys, the corresponding phases and their structure, lattice parameters, magnetic properties are given in Table 1. XRD patterns of the alloy-c in Fig. 1b show a single β-phase structure having B_2 ordering. β-phase transforms to L_{21} ordered structure after annealing at 773 K for 1 h (Fig. 1b). The inset in Fig. 1b confirms the second order $\beta \rightarrow L_{21}$ transition and represents a step after isothermally holding the sample at 773 K for 1 h in DSC.

The microstructure of alloy-a and alloy-b shown in SEM electron back scattered images (Fig. 2a, b) demonstrates that γ-phase has a dendritic morphology and that austenite forms as the inter-dendritic phase. In Ni_2FeGa Heusler alloys, γ-phase forms as the primary phase and austenite as the secondary phase [12]. Large grains of β-phase can be seen in the SEM images in Fig. 2c, d and the appearance of

Table 1 Structural, magnetic and phase transformation properties of Ni_2FeGa Heusler alloy

Ni–Fe–Ga Heusler alloys	Composition (at.%)	e/a ratio	Lattice parameter of austenite	(Å) γ-phase	M at 300 K ($4\pi \times 10^{-7}$ A m^2 kg^{-1})	T_m (K)
Alloy-a	$Ni_{50}Fe_{25}Ga_{25}$	7.75	5.75	3.60	42.18	–
Alloy-b	$Ni_{52}Fe_{25}Ga_{23}$	7.89	5.72	3.58	44.26	225
Alloy-c	$Ni_{49}Fe_{25}Ga_{26}$	7.68	5.74	–	45.32	–
			4.10 (β-phase)		41.16	

Heusler alloy composition is in at.% taken from SEM EDX analysis, lattice parameters of austenite and γ-phase are in aungstrom unit (Å), magnetization (M) at 300 K in ($4\pi \times 10^{-7}$ A m^2 kg^{-1}), martensitic transformation temperature (Tm) in kelvin (K)

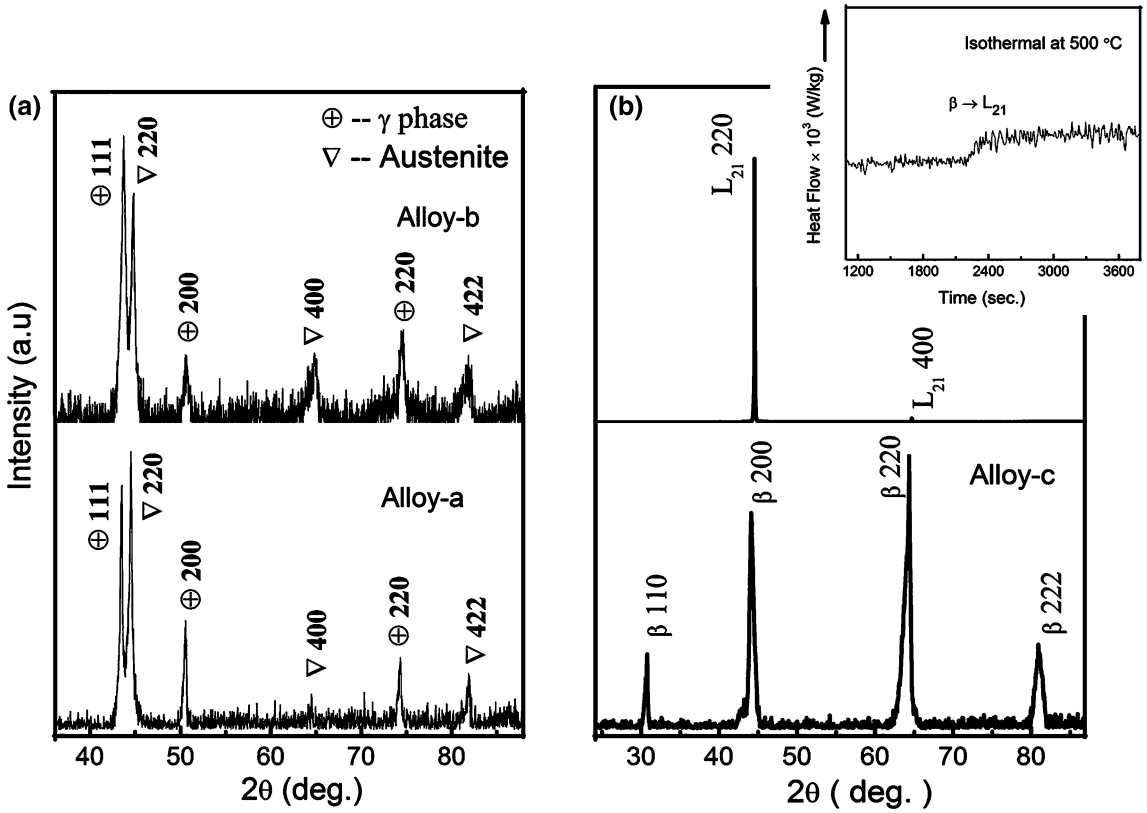

Fig. 1 X-ray diffraction of **a** two phase microstructure of alloy-a and alloy-b showing both fcc and L_{21} structure of γ-phase and austenite respectively, **b** B_2 ordered structure of β-phase in alloy-c which transforms to L_{21} structure after annealing at 773 K for 1 h. *Inset* shows β → L_{21} ordered transformation

sub-grains inside the large grains (Fig. 2d) may be attributed to the short range ordering that take place in the alloy-c. There is fair possibility of the presence of anti-site disorder in the structure due to off-stoichiometric composition as evident from EDX analysis (Table 1). The alloy is slightly deviated from stoichiometry and maintains the alloy composition as $Ni_{49}Fe_{25}Ga_{26}$.

TEM bright field images of both γ-phase and austenite in alloy-a are shown in Fig. 3 along with their corresponding electron diffraction patterns. The dendritic morphology of γ-phase and the inter-dendritic austenite phase can be seen distinctly in Fig. 3a, d. Their corresponding diffraction patterns are indexed as fcc and L_{21} respectively in Fig. 3b, c. The presence of the highly intense 220 spot in Fig. 3c as compared to other visible spots can be attributed to the atomic ordering in the structure. Similarly, the presence of both the phases along with their phase interface in alloy-b are shown in TEM images (Fig. 4b) and their corresponding selected area diffraction patterns are shown in Fig. 4a, c. Tweed structures can be seen in austenite phase and the same has been represented as the diffuse satellite spots around the main diffraction spot in Fig. 4c. Appearance of tweed structures, a pre-martensitic phenomenon, is common in ferromagnetic shape memory alloys and is known to act as potential nucleation sites for martensitic transformation [13]. Figure 4d shows the TEM image of β-phase in alloy-c and the same has been indexed in the diffraction pattern as bcc structure (Fig. 4e).

The isothermal magnetic properties of all the alloys at room temperature are shown in Fig. 5a, b. All the alloys show similar magnetic properties viz, a soft ferromagnetic behavior with similar magnetization values at room temperature. This can be attributed to the similar Fe-content in all the alloys. The magnetization of alloy-c slightly increases after annealing at 773 K demonstrating the atomic ordering β → L_{21} (Table 1). As ordering takes place, Fe occupies the Y-lattice position and Ga occupies the Z-lattice position in L_{21} structure rather than Fe and Ga being randomly distributed between Y and Z lattice positions in the B_2 structure. The magnetic moment in Heusler alloys of X_2MnZ composition are considered to be localized in Mn-atomic sites and contributes mainly to the total magnetic moment [14]. Extending the similar analogy in Ni_2FeGa Heusler alloy, the presence of Fe-atoms at Y-lattice positions mainly contribute to the magnetic properties and the same has been predicted from first principle calculation by Liu et al. [15].

The thermal analysis does not show any phase transition occurring in the temperature range of 148–373 K (−125 to

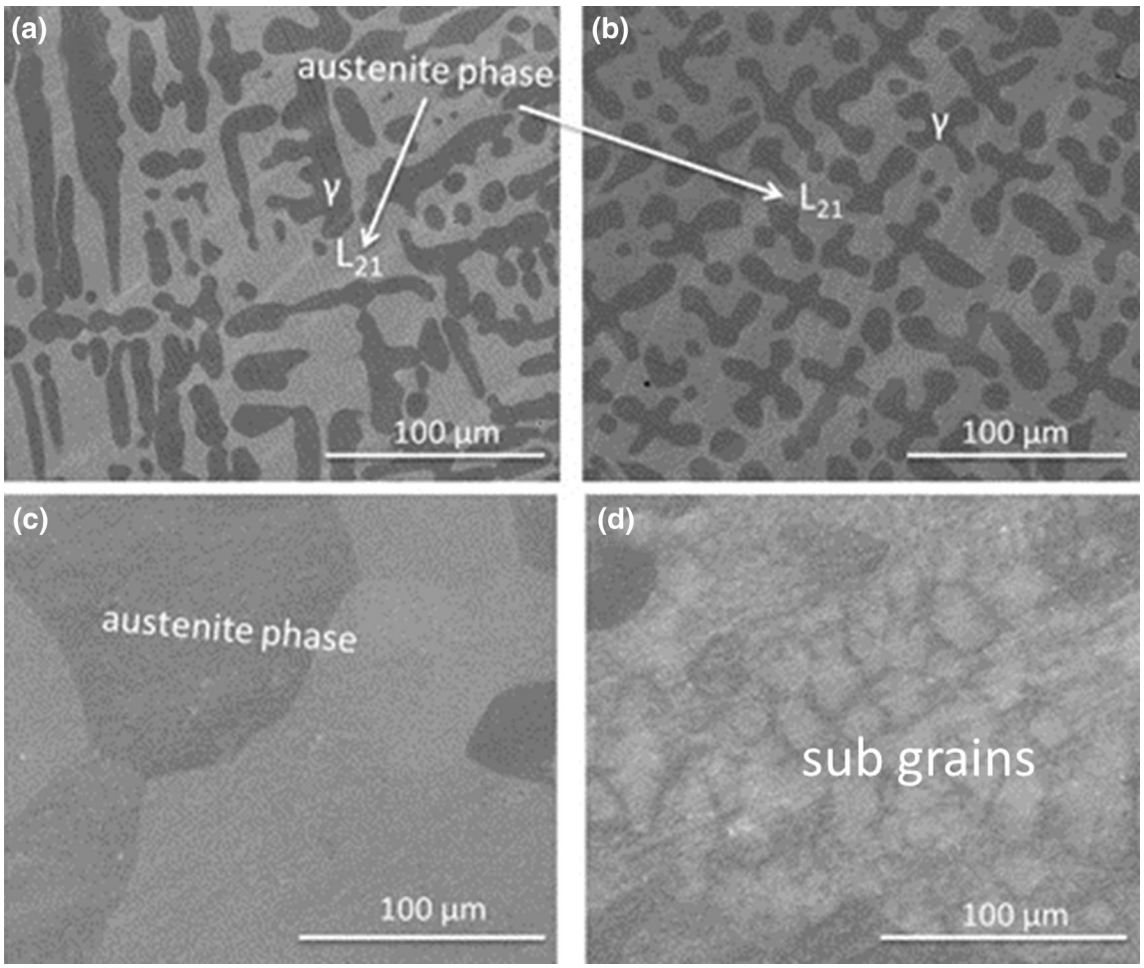

Fig. 2 Electron back scattered SEM images of **a** alloy-a, **b** alloy-b showing dendritic γ-phase and interdendritic austenitic phase in the microstructure, **c**, **d** single phase austenitic microstructure in alloy-c

+100 °C) for the alloy-a and alloy-c. But reversible martensitic transformation is observed for alloy-b at 225 K in DSC results (Fig. 6a). Electrical resistivity exhibits a jump at martensite transformation temperature (220 K) while cooling (Fig. 6b) and resistivity drops at 211 K while heating because of reverse martensite transformation. This sudden change in resistivity is due to the structural phase transformation with an associated hysteresis. The temperature dependency of resistivity follows a different path below and above the transformation temperature indicating a structural transition.

4 Discussion

4.1 Effect of Alloy Composition on Phase Formation

Though the composition of the alloys under study are close to Heusler composition (X_2YZ), alloys a and b have two phase microstructure and alloy c has single phase microstructure. Extensive study of phase and microstructure evolution in Ni_2FeGa Heusler alloy by authors [12] shows that the alloy forms two phase microstructure (γ-phase and austenite) up to 215 K undercooling. Another study [16] showed that higher amount of Ga content in alloy composition stabilizes the austenite phase in Ni_2FeGa Heusler alloy. Thus, the formation of single phase microstructure in alloy-c can be due to the combining effect of higher Ga-content, the quenching effect and large undercooling associated with the chilled copper hearth used for the casting of metal alloy in arc melting furnace. This is very similar to the formation of single phase austenite Ni_2FeGa ribbons by melt spinning [17]. Melt spinning technique is efficient in producing the required undercooling within few microns thickness of ribbons and high thermal conductivity of copper wheel [13]. Arc melting technique produces bulk samples and opens up opportunities for several characterization studies.

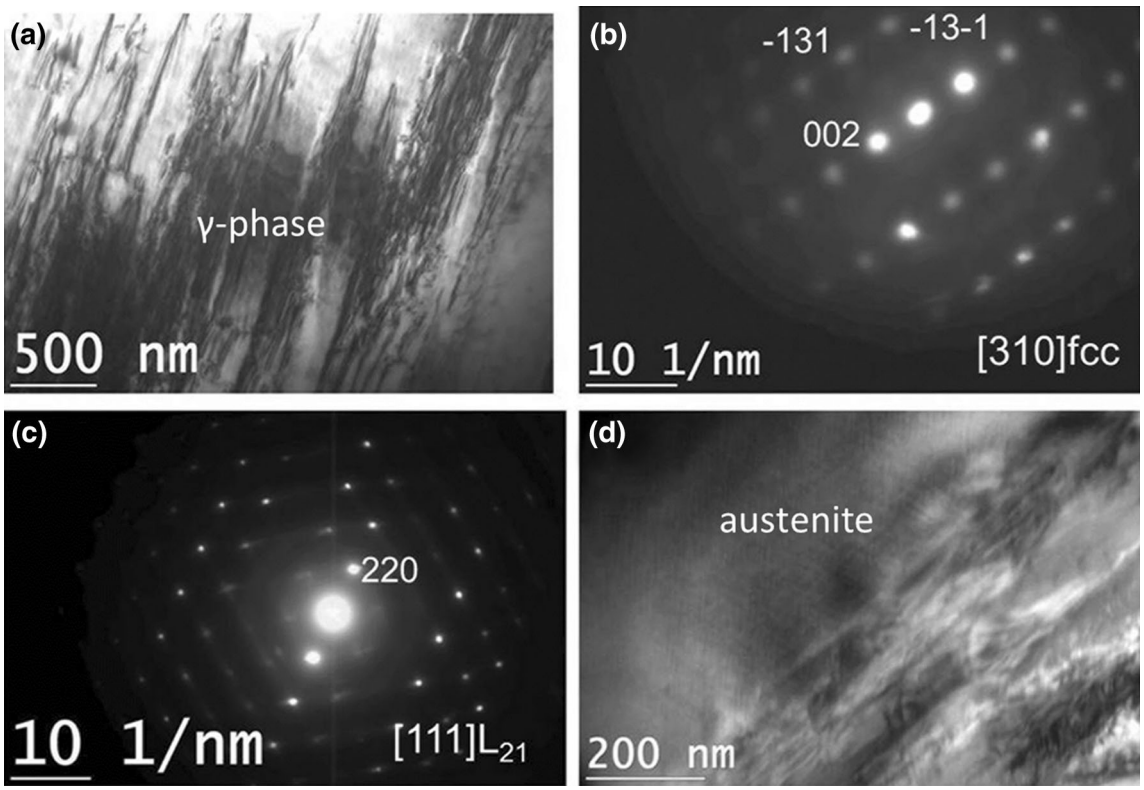

Fig. 3 **a** TEM bright field image of dendritic γ-phase, **b** corresponding diffraction pattern of fcc structure of γ-phase, **c** diffraction pattern of L_{21} structure of austenite in alloy-a and **d** large grain of austenitic phase

4.2 Martensite Transformation

The occurrence of martensitic transformation in alloy-b may be attributed to high Ni-content of the alloy which increases the transformation temperature. It is believed that it is mainly Ni that decides the lattice parameter and affects the structural unit cell of austenite in Heusler alloys [18]. The magnetic properties of all the Heusler alloys a, b and c are quite similar due to similar Fe content in respective alloy compositions. Thus, It is unlikely that the structural transition in alloy-b is of magnetic in origin as there is not sufficient difference in their magnetization values. Excess of Ni in alloy-b can occupy either Fe or Ga lattice sites and can modify the electronic distribution in the density of states near Fermi level. It is reported elsewhere [11] that increase in e/a ratio with substitution of Co in Ni–Mn–Ga Heusler alloy, increases the martensite transformation temperature. The same analogy can be applied in case of alloy-b with higher Ni-content which increases e/a ratio (see, Table 1), which can be the possible explanation for the rise in martensite transformation temperature.

The temperature dependence of resistivity of a metal can be expressed as follows.

$$\rho = \rho_0(1 + \alpha T) \quad (1)$$

α is the temperature coefficient of resistivity which is linear for a metal. Resistivity of austenite and martensite show metal-like behavior, as slopes of these two curves are quite linear as shown in Fig. 6b (except the transformation region). The temperature dependent resistivity below and above transformation temperature show strong dependency of αT term. This indicates that the electrical transport properties of both the phases are due to strong electron–phonon scattering. In case of austenite, the slope of temperature dependent resistivity curve is higher (1.64×10^{-6}) than that of martensite (1.15×10^{-6}). This higher value is obvious at high temperature because the rate of change in resistivity becomes faster as temperature increases due to higher rate of phonon scattering. Once the martensite transformation gets over, the resistivity decreases as temperature decreases and follows a linear trend exhibiting metal like behavior with a lower slope than that of austenite.

According to Matthiesen's rule, the resistivity of a metal can be attributed either to impurities and lattice defects called residual resistivity or due to lattice vibration. The total resistivity is the sum of residual resistivity and contribution due to lattice vibration.

$$\rho = \rho_{residual} + \rho_{lattice} \quad (2)$$

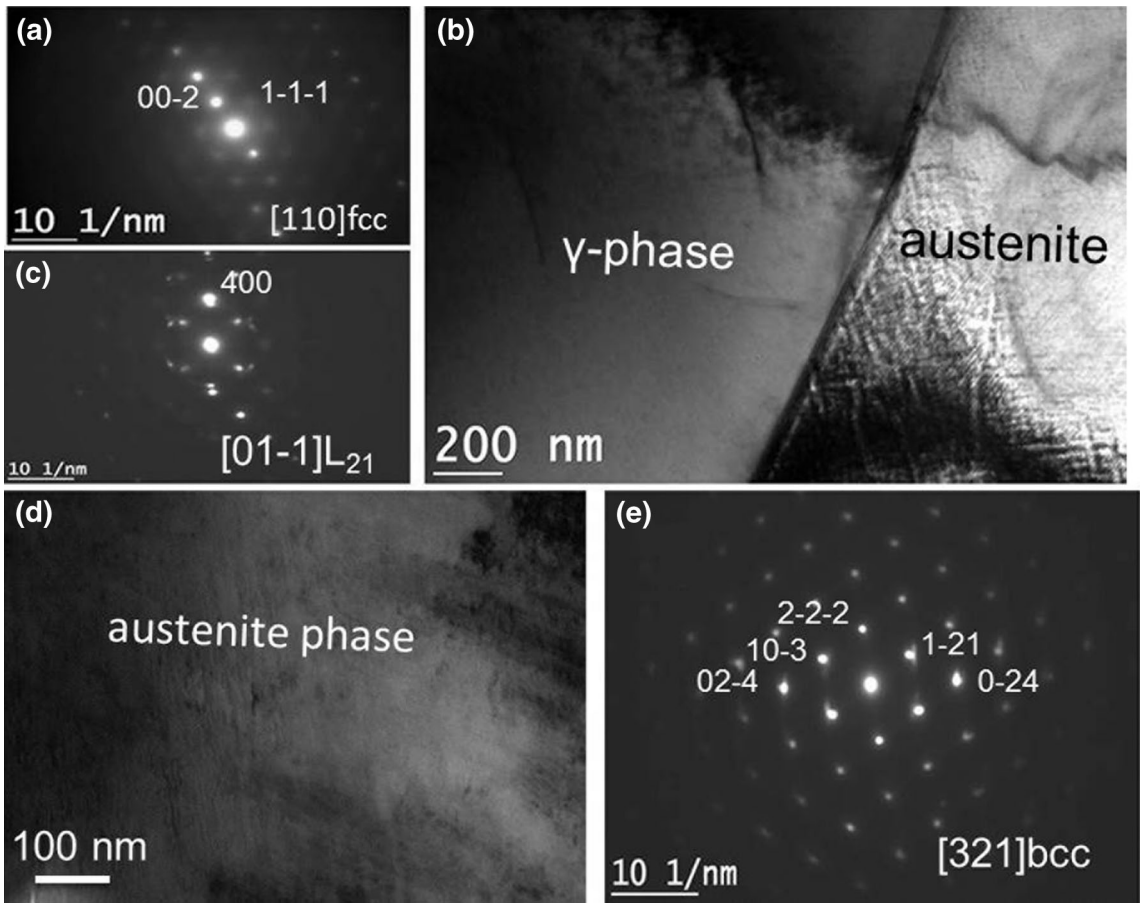

Fig. 4 **a** TEM diffraction pattern of fcc structure of γ-phase, **b** TEM bright field images of both γ-phase and austenite along with their phase interface in alloy-b, **c** L_{21} structure of austente in alloy-b, **d** austenite in alloy-c and **e** the corresponding diffraction of B_2 ordered structure of austenite

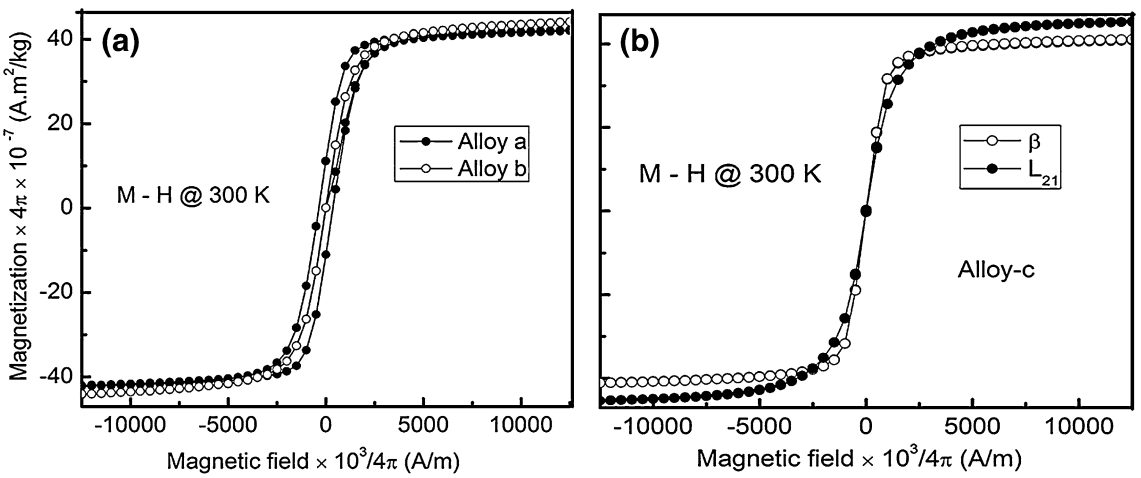

Fig. 5 Magnetic properties of Ni_2FeGa Heusler alloys studied at room temperature: magnetization of **a** alloy-a and alloy-b **b** alloy-c for both the structures (β and L_{21})

A defect structure increases the electron scattering centers and reduces the mean free time between successive electron collisions, thus increasing the resistivity. But the interaction of lattice defects is one of the possible reason for the nucleation of martensite in Heusler alloys [13]. Hence it is expected that defect concentration is annihilated

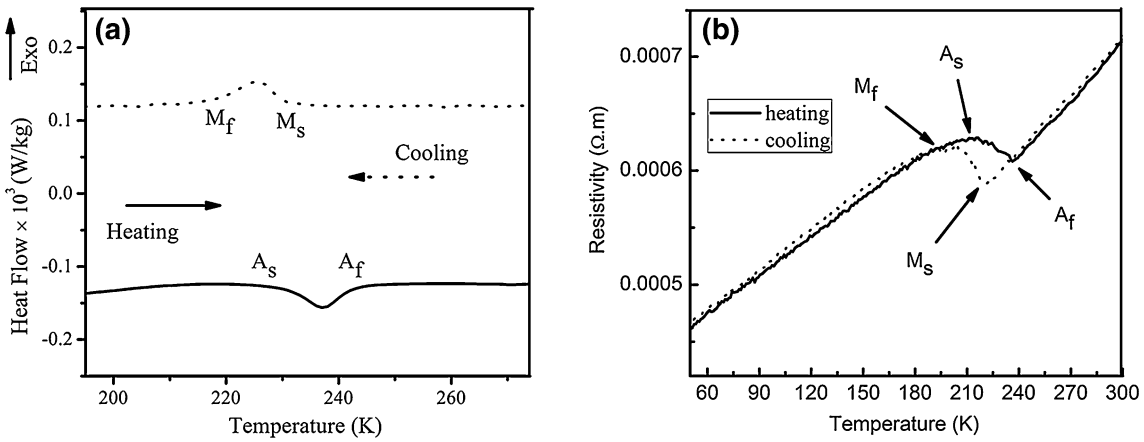

Fig. 6 **a** DSC thermal analysis *curves* showing reversible martensite transformation and **b** temperature dependent resistivity *curves* showing the same for alloy-b

upon martensite transformation. The role of defects in the increase in resistivity upon martensite transformation is suspected. The effect of lattice vibration is also neglected as martensite is a low temperature phase and lattice vibration is supposed to be negligible at low temperature.

The rise in resistivity upon martensite transformation may be due to two reasons e.g., due to change in scattering centers or due to the modification of effective electron concentration. Scattering centers are related to the defect structure of martensite, which is not expected and martensite too has a periodic lattice configuration. Martensite twin variants and twin boundaries can act as the source of electron scattering and can increase the resistivity.

Effective mass (m^*) of electron is not constant. It depends on the geometry of the energy states at Fermi level. m^* is related to the term which represents the extent up to which an electron can behave as a free electron. If effective mass of free electron in martensite (m^*_{mart}) is higher, the mobility of free electron is constrained, and hence it increases the resistivity. At the same time if the number of free electrons available is less, that also increases the resistivity.

The common explanation in band theory is that when a crystal deforms, the degree of overlapping of orbitals changes which increases the width of energy bands. If the increase in band width of degenerate energy levels in martensite is to be believed, then it can be attributed to the different crystal symmetry of martensite which modifies the density of states and the electronic distribution. Martensitic transformation in Ni–Mn–Ga Heusler alloys was explained using the band Jahn–Teller mechanism [19] by splitting of degenerate energy levels. As temperature is lowered, the electronic structure gets redistributed and forms a low energy state martensite by structural transition. But in case of Ni_2FeGa Heusler alloy, as per the published report [20] suggests, Ni-e_g and Fe-t_{2g} states converge. They form two low lying t_{2g} hybridized states one below and one above the Fermi level which lowers the total energy and stabilizes martensite phase. High density electronic states are also observed below and above the Fermi level for both the parent and product phases in Ni_2FeGa Heusler alloy [20]. A change in m^*_{mart} is expected due to the possible change in geometry of the energy states. Most probably m^*_{mart} is higher than m^*_{aus} (effective mass of free electron in austenite) so that electron in martensite state behaves as a heavy particle and can contribute to the increase in resistivity upon martensite transformation. The same suggestion was made by Sahariah et al. [20] who studied the Fermi surface topology to understand martensite transformation in Ni_2FeGa Heusler alloy.

5 Conclusions

1. The alloys possessed two-phase microstructure having both fcc and L_{21} structures. Alloy-c was formed as single β-phase due to the combining effect of higher Ga content and quenching effect. β-phase later get transformed to L_{21} ordered structure upon annealing. All the alloys studied had 25 at.% of Fe which gave similar magnetic properties. Increase in magnetization was observed due to β to L_{21} order transformation in alloy-c.
2. Martensitic transformation in alloy-a and alloy-c was not observed in the temperature range of 148–373 K. The martensite transformation temperature might lie below 148 K in these alloys. In case of alloy-b, martensite transformation temperature was noticed at 225 K which was attributed to higher Ni-content replacing Ga as compared to the other two alloys.
3. Temperature dependent electrical resistivity of both austenite and martensite phases were attributed to

strong electron–phonon scattering. The rise in resistivity upon martensite transformation was attributed to the change in effective mass of electron due to phase transition to a low symmetry structure.

4. This investigation emphasized on the deep understanding of geometry of the Fermi surface to understand martensite transformation in Ni_2FeGa Heusler alloys and created scope for future investigation.

Acknowledgments Authors like to thank Prof. P. N. Santosh, Prof. R. Nirmala, Dr. Ganesh Raj and Mr. Rajib Mondal, Department of Physics IIT Madras for their kind help in resistivity measurement.

References

1. Huang Y J, Hu Q D, Bruno N, Karaman I ,and Li J G, *Mater Lett* **114** (2014) 11.
2. Biswas A, Singh G, Sarkar S, Krishnan M, and Ramamurty U, *Intermetallics* **54** (2014) 69.
3. Qian J F, Zhang H G, Chen J L, Wang W H, and Wu G H, *J Crystal Growth* **388** (2014) 107.
4. Sánchez-Alarcos V, Pérez-Landazábal J I, Recarte V, RodríguezVelamazán J A, and Chernenko V A, *J Phys Condens Matter* **22** (2010) 166001.
5. Xuan H C, Xie K X, Wang D H, Han Z D, Zhang C L, Gu B X, and Du Y W, *Appl Phys Lett* **92** (2008) 242506.
6. Heczko O, Fahler S, Vasilchikova T M, Voloshok T N, Klimov K V, Chumlyakov Y I, and Vasiliev A N, *Phys Rev B* **77** (2008) 174402.
7. Aich S, Das S, Al-Omari I A, Alagarsamy P, Chowdhury S G, Chakraborty M, Shield J E, and Shellmyer D J, *J Appl Phys* **105** (2009) 07A943.
8. Liu Q H, Liu J, Huang Y J, Hu Q D, and Li J G, *J Alloys Compd* **571** (2013) 186.
9. Sehitoglu H, Wang J, and Maier H J, Inter. *J Plast* **39** (2012) 61.
10. Sharma V K, Chattopadhyaya M K, Kumar R, Ganguli T, Kaul R, Majumdar S, and Roy S B, *J Phys D Appl Phys* **40** (2007) 3292.
11. Prasad R V S, Raja M M, and Phanikumar G, *Intermetallics* **25** (2012) 42.
12. Nath H, and Phanikumar G, *Mater Sci Forum* **790–791** (2014) 199.
13. Prasad R V S, Srinivas M, Raja M M, and Phanikumar G, *Metall Mater Trans A* **45** (2014) 2161.
14. Chatterjee S, Singh V R, Deb A K, Giri S, De S K, Dasgupta I, and Majumdar S, *J Magn Magn Mater* **322** (2010) 102.
15. Liu Z H, Hu H N, Liu G D, Cui Y T, Zhang M, Chen J L, Wu G H, and Xiao G, *Phys Rev B* **69** (2004) 134415.
16. Nath H, and Phanikumar G, doi:10.1007/s 11661-015-3098-7.
17. Liu Z H, Zhang M, Cui Y T, Zhou Y Q, Wang W H, Wu G H, Zhang X X, and Xiao G, *Appl Phys Lett* **82** (2003) 424.
18. Graf T, Casper F, Winterlik J, Balke B, Fecher G H, and Felser C, *Z Anorg Allg Chem* **635** (2009) 976.
19. Brown P J, Bargawi A Y, Crangle J, Neumann K U, and Ziebeck K R A, *J Phys Condes Matter* **11** (1999) 4715.
20. Sahariah M B, Ghosh S, Singh C S, Gowtham S, and Pandey R, *J Phys Condens Matter* **25** (2013) 025502.